Child's Nervous System (2019) 35:129–137
https://doi.org/10.1007/s00381-018-3935-2

ORIGINAL PAPER

Diffusion tensor imaging (DTI) and Tractography of the spinal cord in pediatric population with spinal lipomas: preliminary study

Pierre Antherieu[1] · R. Levy[2] · T. De Saint Denis[3] · L. Lohkamp[4] · G. Paternoster[3] · F. Di Rocco[4] · N. Boddaert[2] · M. Zerah[3]

Received: 20 April 2018 / Accepted: 25 July 2018 / Published online: 2 August 2018

Abstract

Purpose Diffusion tensor imaging (DTI) allows studying the micro and macro architecture. One of the major challenges in dysraphism is to know the morphologic organization of the spinal cord. In a preliminary work, spinal lipoma was chosen for analyzing the micro-architecture parameters and fiber morphology of the spinal cord by DTI with tractography.

Methods Twelve patients (0–8 years) related to spinal lipomas treated between May 2017 and March 2018 were included. Tractography reconstruction of the conus medullaris of 12 patients were obtained using the MedINRIA software. The diffusion parameters have been calculated by Osirix DTImap plugin.

Results We found a significant difference in the FA ($p = 0.024$) between two age groups (< 24 months old and > 24 months old). However, no significant differences in the mean values of FA, RD, and MD between the level of the lipoma and the level above were noted. The tractography obtained in each case was coherent with morphologic sequences and reproducible. The conus medullaris was deformed and shifted. Destruction or disorganization of fibers and any passing inside the lipomas was not observed.

Conclusions Tractography of the conus medullaris in a very young pediatric population (0–8 years old) with a spinal lipoma is possible, reproductive, and allows visualization of the spinal cord within the dysraphism. Analysis of the FA shows that the presence of a lipoma seems to have an effect on the myelination of the conus medullaris. It is during the probable myelination phase that the majority of symptoms appear. Is the myelination per se the cause?

Keywords Diffusion tensor imaging · Fiber tractography · Spinal dysraphism · Conus medullaris · Spinal lipomas

Introduction

Spinal dysraphisms represent a heterogeneous group of malformations of spinal development encountered in pediatric neurosurgery [1]. In this heterogeneous group of malformations, Spinal lipomas (SL) are among the most common forms of closed neural defects, with a minimal incidence of 4–8 per 100,000, clearly under evaluated [2]. One of the current challenges in SL is to know the natural history of these diseases for choosing the optimal time point for surgery [3], because a prophylactic surgery is currently discussed controversially in asymptomatic patients. We do not know the impact that a dysraphism can have on the myelination and the microstructure of the spinal cord and if there exists an associated spinal cord dysplasia.

Until now, there exist no noninvasive routine clinical techniques for visualizing the spinal cord organization in dysraphisms beyond the classical morphological sequences of magnetic resonance imaging (MRI) (mostly T1 and T2) and ultrasound. Diffusion tensor imaging (DTI) is a relatively new MRI technique, which is sensitive to the random movement of water molecules in tissue "in vivo" [4]. The microarchitecture of the white matter with a main orientation direction of the fibers caused a high degree of anisotropy in the random movement [5, 6].

✉ Pierre Antherieu
pierreantherieu@wanadoo.fr

[1] Department of Neurosurgery, University Medical Center, Avenue Albert Raimond 42270 Saint Priest en Jarez, Saint Etienne, France

[2] Department of Pediatric Radiology, Necker –Enfants Malades's Medical Center, Paris, France

[3] Department of Pediatric Neurosurgery, Necker –Enfants Malades's Medical Center, Paris, France

[4] Department of Pediatric Neurosurgery, University Medical Center, Lyon, France

Fractional anisotropy (FA) and other parameters of diffusivity reflect the microstructure of the white matter as their modifications reflect abnormalities beyond the resolution of conventional anatomic MRI sequences [7]. The FA corresponds to the degree of directional dependence, whereas the mean diffusivity (MD) reflects the average of diffusion, the radial diffusivity (RD), the part of diffusivity perpendicular to fibers, and the axial diffusivity (AD), the part of diffusivity parallel to the fibers in the spinal cord. The fiber tractography (FT) is a virtual reconstruction of the fibers itself and their orientation in the white matter by mathematic models.

Consequently, DTI and FT are noninvasive techniques to study the 3D architecture of the white matter in the brain and in the spinal cord in vivo. DTI has generated a lot of studies and clinical applications in the brain, in particular for neurosurgical purposes [8, 9]. More recently FT was applied to the spinal cord and most importantly in the cervical cord [10, 11]. Very few papers in the literature have studied its application to the thoracic or lumbar spinal cord and meanly in adult population [10–13]. In the condition of dysraphism, only three teams have published a study [12, 14, 15], and we have not found any feasibility studies in dysraphism for a very young pediatric population (0 to 8 years). Saksena et al. studied the feasibility of the DTI on the whole spinal cord in healthy children but only after 6 years [16]. Yet it is during this very young age that medical problems appear, and finally the limited size of the pediatric spinal cord and process of myelination have not been studied.

Before proposing a large study for analyzing the spinal cord by DTI with FT in children with multiple forms of dysraphism, (The aims would be to better understand the architecture and organization of the spinal cord including its fiber tracts and eventually to propose a classification based on these new techniques.), we assessed in this study, the clinical feasibility and preliminary results of DTI (with FT) in the spinal cord and the conus medullaris, focusing on a single pathology: spinal lipomas. We have chosen to study in a first intention the SL in children aged 0 to 8 years old as it represents the most common form of dysraphism.

The FA and the different diffusivities (MD, RD, and AD) were analyzed for better understanding of the micro-architecture and myelination of the thoraco-lumbar cord in children presenting with a SL. We also realized tractography reconstructions seeking to improve the macro-architecture knowledge.

Materials and methods

Study population and data acquisition

All children, seen for a follow-up of SL at the neurosurgical clinic between May 2017 and March 2018, underwent a routine MRI in the radiology department of Necker-Enfants Malades in Paris and were included in this prospective study. We recovered their clinical and DTI datasets. The patients who have already had spinal surgery and whose MRI did not include DTI sequences as well as those who were contra-indicated for MRI have been excluded from our study. Patient characteristics, clinical symptoms, and the type of lipoma were retrieved and are summarized in Table 1. Twelve patients (5 males and 7 females, median age 41.92 months, range 2–95 months) with or without symptoms (2 asymptomatic, 7 neurological symptoms, 4 orthopedics complications, 6 skin signs, 0 pain, 8 vesico-sphincter disorders) related to SL were included. (Table 1).

The MRI protocol used in the radiology department for spinal cord imaging was applied with a 3 Tesla MR system (Discovery MR750; GE Médical Systems, USA) using a 16-channel phased-array surface coil and included a DTI sequence. The diffusion tensor sagittal images were acquired with a single-shot spin echo diffusion-weighted spin echo planar imaging (EPI) with the following parameters: TE = 60 ms; TR = 1500 ms; FOV 26 mm^2; matrix size 100 × 3, 16 slices thickness = 4 mm; resolution voxel size 1,0156 × 1,0156 × $4mm^3$; *b* values = 0 and 1000 s/mm^2, and 30 gradient directions. The total acquisition time of the DTI sequence was 6.5 min. Diffusion weighting was implemented using a Stejskal-Tanner diffusion scheme. The DTI sequence was positioned to the thoracolumbar level.

Two additional morphologic sequences were used: 3D T1weighted images (TR = 820 ms; TE = 13,652 ms; voxel size 0.625 × 0.625 × $0.499ms^3$; 152 slices) and sagittal T2-weighted images. (TR = 2500 ms; TE = 124,74 ms; voxel size 0.5078 × 0.5078 × $3mm^3$; 14 slices).

Data processing and analyses

The DTI datasets were post-processing analyzed by the MedINRIA software v.2.2.3 Inria Copyright 2013. [17] This software is using a itkProcessTensorLogEclidean plugin for fiber tractography reconstruction with the LogEclidean algorithm [18]. The plugin performs a total volume FT reconstruction of the DTI acquisition, and based on these data, the useful reconstructions were selected. Regions without interest were deselected by categorizing them as "NOT." We have chosen to keep the reconstruction of the region including the medullary cone, enlarged to the upper vertebral level and including intra-spinal lipoma. The level of the dysraphism has been identified from the 3D T1 sequence. The parameters of FT LogEclidean reconstructions were Starting FA threshold = 200, stopping FA threshold = 300, smoothness = 20, minimum length = 1 and sampling = 1. Color encoding of the reconstructed fibers were chosen as a standard color code used in the brain: blue indicating the cranio-caudal, green the

Table 1 Individual patient characteristics, clinical symptoms, and lipoma type

	Age (months)	Sex	Symptoms						Lipomas type
			Motor and sensory	Orthopedics symptoms	Bladder	Bowel	Pains	Skin signs	
1	8	F	Deficit	Foot deformity	–	–	–	–	Lipomyelocystocele
2	95	M	–	–	Dysuria	Incontinence	–	–	Terminal
3	86	M	Reflex abolition	–	Dysuria	Constipation	–	Deviation of the gluteal fold	Terminal
4	66	F	–	–	Neurological bladder	–	–	Skin defect	Transitional
5	7	F	–	–	–	–	–	Subcutaneous lipoma + angioma	Transitional
6	9	M	Deficit	Foot deformity	Neurological Bladder	–	–	–	Lipomyelocystocele
7	29	F	Distal deficit	–	–	–	–	Subcutaneous lipoma	Lipomyelocystocele
8	39	M	Distal deficit	Foot and leg deformity	–	–	–	–	Dorsal
9	83	M	–	–	Dysuria	–	–	Subcutaneous lipoma	Dorsal
10	2	F	–	–	–	–	–	–	Lipomyelocystocele
11	38	M	Reflex abolition	Foot deformity	Dysuria	–	–	–	Lipomyelocystocele
12	50	F	Distal deficit	–	Neurological bladder	Incontinence	–	Subcutaneous lipoma	Terminal

antero-posterior, and red the left-right direction. The intermediate colors correspond to oblique directions.

The diffusion parameters (FA, MD, AD, and RD) have been calculated by Osirix v.9.0 (http://www.osirix-viewer.com) and DTImap plugin. Quantitative measurements of diffusion parameter values were obtained by positioning the region of interest (ROI) in the sagittal plan of FA map. Three measurements were made on the vertebral level above the lipoma and four measurements were performed at the level of the SL itself.

Statistical analysis

The FA, MD, AD, and RD mean values of the lipoma level and the level above were compared by *t* test. In addition, a *t* test was also realized to compare the difference of diffusion parameters between two age groups (< 24 months and > 24 months). A p value < 0.05 was considered as significant. The statistical analysis was performed using the commercially available software SPSS version 20 (IBN, Chicago, USA).

Results

Parameters of diffusivity

FA, MD, AD, and RD measurements were realized for all children, four measurements on the spinal cord at the lipoma level and three measurements at the level above. The mean global FA, MD, AD, and RD values at the level of the pathology were 0.335 ± 0.038, 0.139 ± 0.010, 0.190 ± 0.009, and 0.115 ± 0.011 mm^2/s respectively, and the mean global values for level above were 0.388 ± 0.031, 0.151 ± 0.009, 0.214 ± 0.010, and 0.119 ± 0.009 mm^2/s respectively. All the results were summarized in Table 2. We found a significant difference in AD diffusivity ($p = 0.008$). However, no significant differences were noted in FA, MD, and RD values between the lipoma level and the level above (all $p > 0.05$).

The additional tests were summarized in Graphs 1 and 2. The *t* test showed a significant difference between the two age groups (< 24 months old and > 24 months old) for the level above the SL. The mean FA values were 0.290 ± 0.02 and 0.46 ± 0.09 respectively for < 24 months and > 24 months ($p = 0.024$), whereas they corresponded to 0.305 ± 0.013 and 0.357 ± 0.014 in the pathological level (with $p = 0.889$).

There were no significant differences in other diffusivity parameters between the two age groups and the two clinical groups observed.

Tractography results

FT of the conus medullaris was feasible in 11 of the 12 children included in our study. In one case, the tracking could not be performed because the DTI data had too many image distortions and motion artifacts. An example of tracking is provided in Fig. 1.

The tractography obtained was coherent with a morphologic sequence of the spinal cord that was additionally visualized in each of the 11 patients. Moreover, the tracking was found to be reproducible.

Table 2 Mean and standard deviation of the diffusion parameters (FA, MD, AD, and RD) at the lipoma level and the level above the lipoma

Age (months)		FA (mm^2/s) × 10^-4		Diffusivity (mm^2/s) × 10^-6					
				MD		AD		RD	
		Mean level Up	Mean lipomas level	Mean level up	Mean lipomas level	Mean level up	Mean lipomas level	Mean level up	Mean lipomas level
1	8	2687 ± 495	3061 ± 355	1781 ± 41	1243 ± 182	2238 ± 17	1662 ± 141	1529 ± 102	1035 ± 81
2	95	4655 ± 958	2606 ± 680	1354 ± 225	1424 ± 123	2115 ± 176	1859 ± 277	973 ± 249	1207 ± 58
3	86	5290 ± 659	3044 ± 464	1226 ± 77	1167 ± 78	2032 ± 11	1531 ± 87	823 ± 111	985 ± 96
4	66	5213 ± 318	6118 ± 748	1595 ± 176	1279 ± 164	2396 ± 239	2213 ± 428	1196 ± 143	813 ± 69
5	7	3151 ± 995	3818 ± 483	1098 ± 282	1124 ± 127	1469 ± 218	1607 ± 102	914 ± 314	882 ± 141
6	9	2834 ± 649	2272 ± 240	1672 ± 48	1811 ± 296	2145 ± 91	2253 ± 361	1435 ± 118	1589 ± 269
7	20	3075 ± 794	4729 ± 644	1424 ± 127	1209 ± 142	1885 ± 225	1890 ± 229	1183 ± 131	868 ± 139
8	39	5655 ± 262	3172 ± 165	1187 ± 168	1336 ± 92	2051 ± 236	1757 ± 165	756 ± 133	1125 ± 591
9	83	3782 ± 816	4654 ± 543	1617 ± 10	1166 ± 38	2311 ± 163	1825 ± 69	1270 ± 98	837 ± 81
10	2	2733 ± 385	1394 ± 538	2100 ± 187	2234 ± 190	2688 ± 198	2547 ± 219	1805 ± 194	2077 ± 206
11	38	4287 ± 519	3252 ± 330	1130 ± 95	1002 ± 179	1677 ± 80	1592 ± 266	857 ± 112	828 ± 139
12	50	3256 ± 291	2110 ± 391	1923 ± 167	1753 ± 147	2628 ± 207	2141 ± 173	1570 ± 156	1559 ± 142

Each time, the fibers were situated in front of the lipoma, no matter what type of lipoma was found, and the conus medullaris was deviated around the lipoma and consecutively shifted to one side. (Figs. 2 and 3) We have not found any destruction or disorganization of the fibers and no fibers passing within the lipoma in the entire cohort. The tractographic reconstructions are also architecturally coherent with Chapman's classification [3].

Discussion

To our knowledge, this is the first study that describes and reflects the feasibility of DTI and fiber tractography in spinal cord lipomas per se as well as in the pediatric population. DTI in the spinal cord, especially in pediatrics, presents some challenges. Firstly, the limited size of the pediatric spinal cord; secondly, movements related to breath, cardiac activity and mostly children's difficulties of cooperation, induce artifacts and may cause some massive images distortions. This is a major cause of deterioration of the quality of DTI reconstruction and analysis [19, 20]. The department of radiology in our center is exclusively dedicated to the pediatric population, and the DTI sequences have been optimized within a specific acquisition protocol in order to decrease motion artifacts. A sagittal slice series and large voxel volumes (1 ×1 × 4 m^3) allow obtaining a short sequence with an average duration of 6.5 min. These sequences are realized in clinical practice

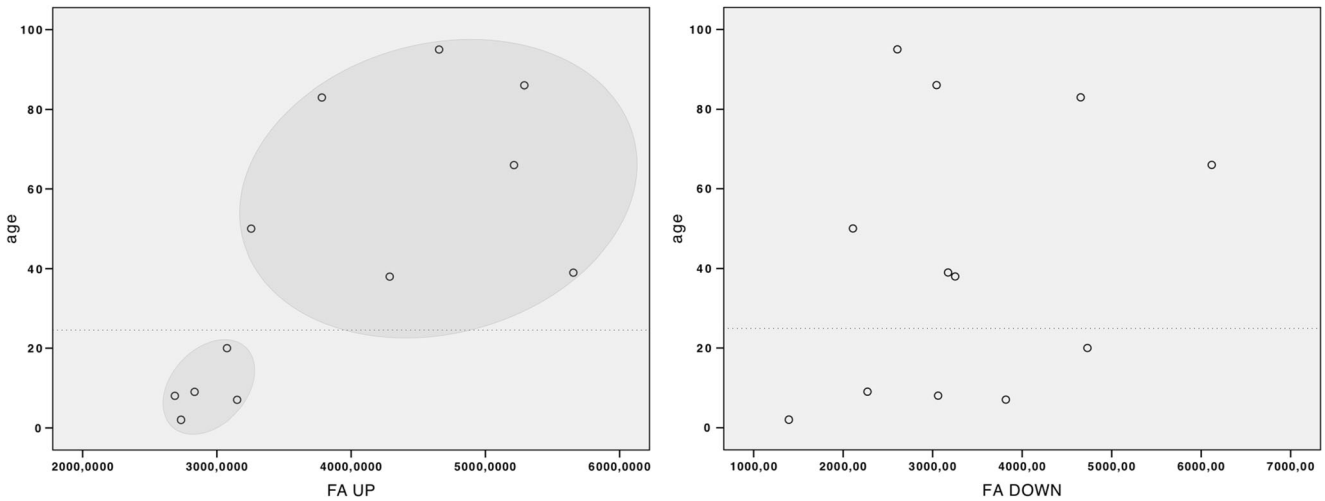

Graph 1 Scatter blots showing FA values correlated to age (months) in the conus medullaris for the lipoma level (FA LIP) and the level above the lipoma (FA UP). The chart suggests that there are two groups in FA UP depending on their age that are no longer present at the level of the lipoma

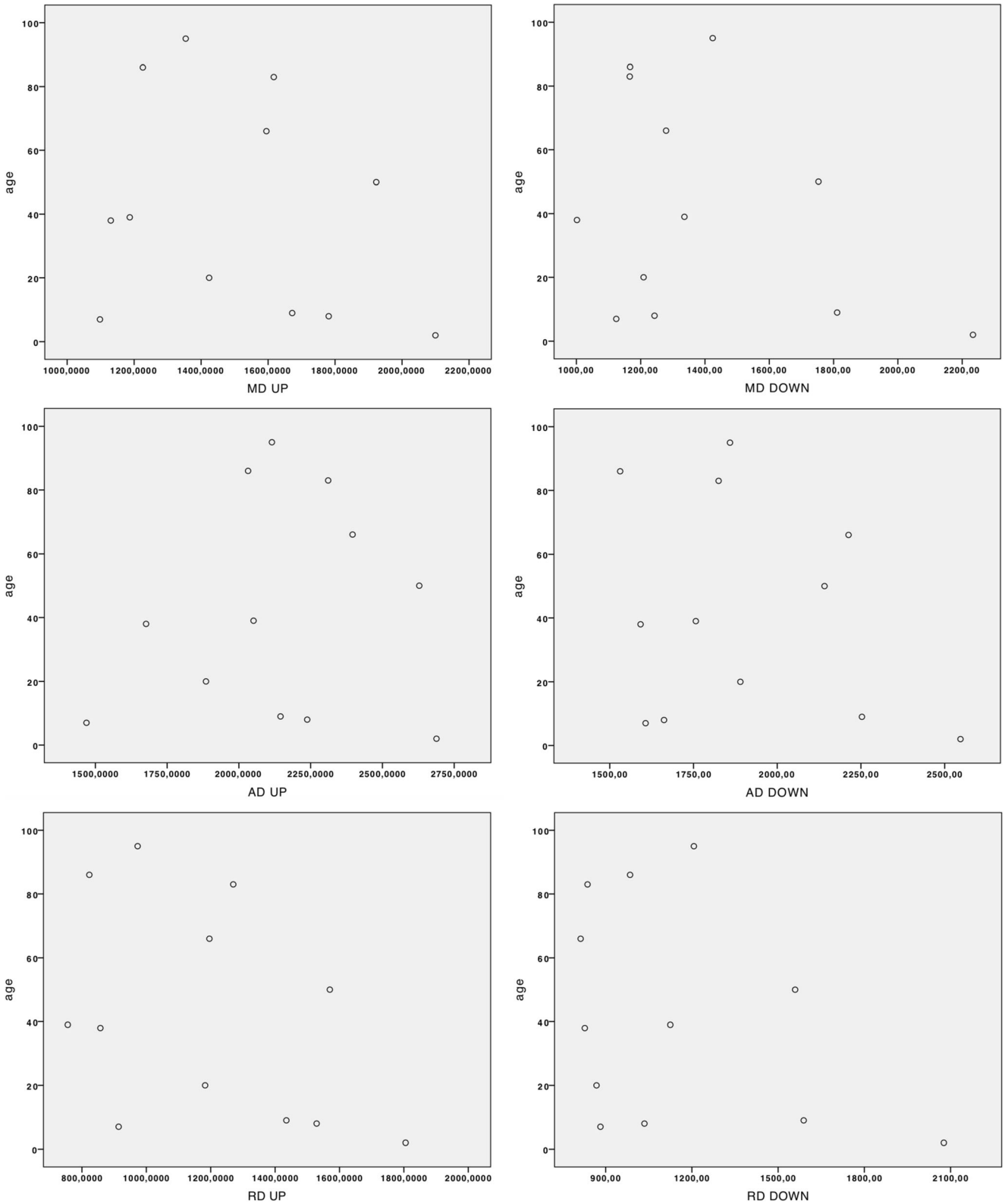

Graph 2 Scatter blots showing the relationship between MD, AD, or RD values and age (months) in the conus medullaris for the lipoma level (LIP) and the level above the lipoma, upper level (UP)

and all the MRI were performed without general anesthesia. However, these criteria of DTI have decreased the quality of data and given the fact that this was a compromise solution, this represents one limitation of this study.

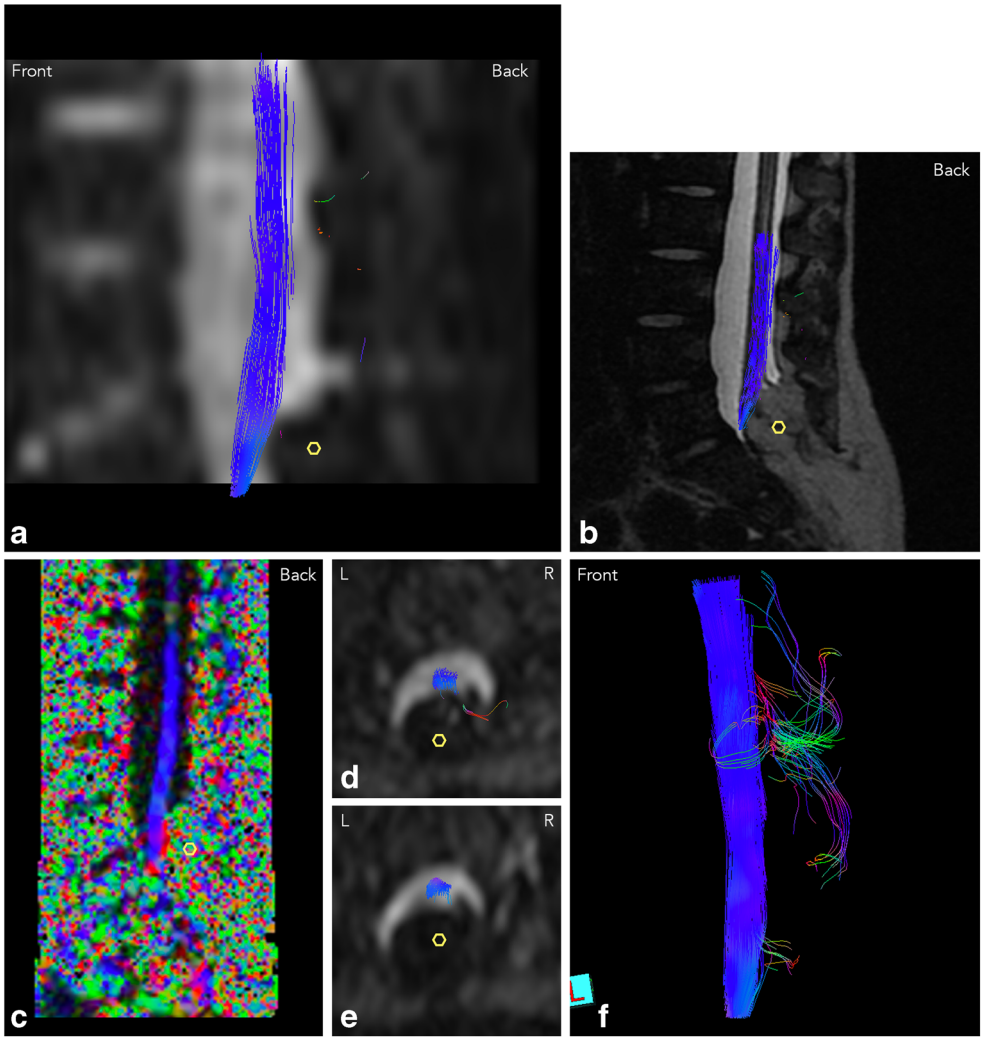

Fig. 1 Tractography reconstruction of patient 11 (male, 38 months old) with a dorsal lipoma indicated by a yellow hexagon. **a** Tractography of the conus medullaris. **b** Tractography of the conus medullaris combined with 3D T2 morphologic MRI sequences. **c** Sagittal FA mapping. **d**, **e** Axial reconstruction. **f** 3D fiber tracking. The conus medullaris is deformed around the lipoma and no fibers were found inside the lipoma

Micro-architecture: diffusivity parameters

We have realized FA, AD, MD, and RD measurements in the spinal cord at the lipoma level and at the level above, notably the first level that was clinically and radiologically normal (without anomalies found on MRI conventional sequences). Seksena et al. showed that the diffusivity values remain relatively stable along the thoracic and lumbar spinal cord [16]. For this reason, we have chosen to compare the diffusivity at the conus level and the level above the pathology, the lipoma respectively.

We did not find any significant difference between these two levels in FA, RD, and MD, which is an interesting point. Perhaps the lipomas do not modify the microarchitecture of the white matter but usually produce a mass effect responsible for modifying the AD that is part of the diffusivity parallel to the fibers. But the limits of our preliminary study do not allow definitive conclusions at this time. In fact, the spinal cord diffusivity values, in particular FA, in children, are very variable according to age and inter-individual [16, 20, 28, 21]. This is probably due to the difference of maturation and myelination of the white matter. Moreover, these parameters are very sensitive to motion artifacts that induce spatial distortion and affect diffusivity measurements and it is a mean problematic with a non-cooperating pediatric population.

The additional analysis of FA shows some trends:

- There is a significant difference between the groups < 24 months (with low FA) and > 24 months (with higher FA) at the healthy level. This can probably be explained by the ongoing process of myelination in the < 24 months group. Dubois (2008), has shown that FA decreases during the active myelination a phase. It is due to a decrease of organization and therefore a sign of anisotropy [22].
- This significant difference is no longer found at the lipoma level.

It is for us the major result of our preliminary work. We could make two hypotheses: Firstly, the major part of the

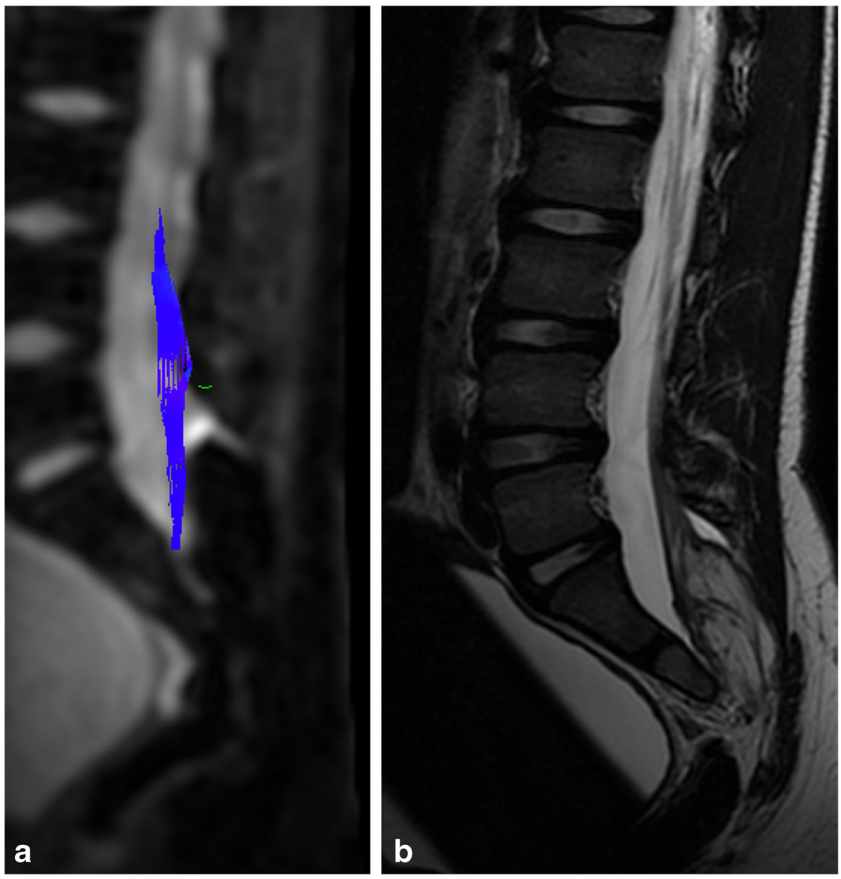

Fig. 2 **a** Partial sagittal reconstruction of the spinal cord in a 95-month-old boy 2 with a terminal lipoma. **b** Sagittal T2 plane

process of myelination is ongoing until the age of 2 years, which goes in line with the observations reported in the literature [23–25], The literature is poor on this subject (PubMed and ScienceDirect), but it is generally accepted that myelination is realized in fetal life and before 2 years of age [24]. But this process may continue until adulthood. Only one paper [16] studies DTI in the conus medullaris in children and this study does not allow us to confirm our hypothesis. Saksena and al. includes indeed only children from 6 to 16 years of age in his study, which excludes comparable patients and results during the supposed myelination period.

Secondly, the presence of a lipoma seems to have an effect on the myelination of the conus medullaris. The differences between the two age groups are lost at the lipoma level. Emerging or worsening clinical symptoms are usually observed before the age of 3 years and we know that after 3 years, the risk of clinical worsening is only 22% [25, 29]. It is therefore during the supposed myelination phase that appears majority of symptoms. SL have a multifactorial pathophysiology [1–3], the results of our study seem to show that a part could be due to the process of myelination, but this alone cannot explain the natural history of this pathology.

Macro-architecture: tractography

To optimize the tracking reconstruction in this very young population, we have used the log-Euclidean algorithm, which relies on a log-Gaussian noise that improves the estimation of DTI in a clinical context [18]. In this manner, all patients were able to receive a tracking of conus medullaris, except one patient, whose tracking results remained compromised by important motion artifacts.

Our preliminary study shows that post-processing tractography reconstructions in the sagittal plan are realizable and coherent with morphologic sequences of MRI, with Chapman's classification and with the per-operative observations [1]. In each case, reproducible images showed that fibers are deviated to the front, and the conus medullaris is deformed around the lipoma. The reconstructions did not confirm any fibers within the lipomas. This is in complete accordance to the peri-operative observations as complete removal of the SL is possible in the vast majority of cases without clinical consequences [1].

Nevertheless, tractography is not a direct fiber by fiber visualization technique, it is a probabilistic construction. In this pathology, it seems interesting to use it by carrying out

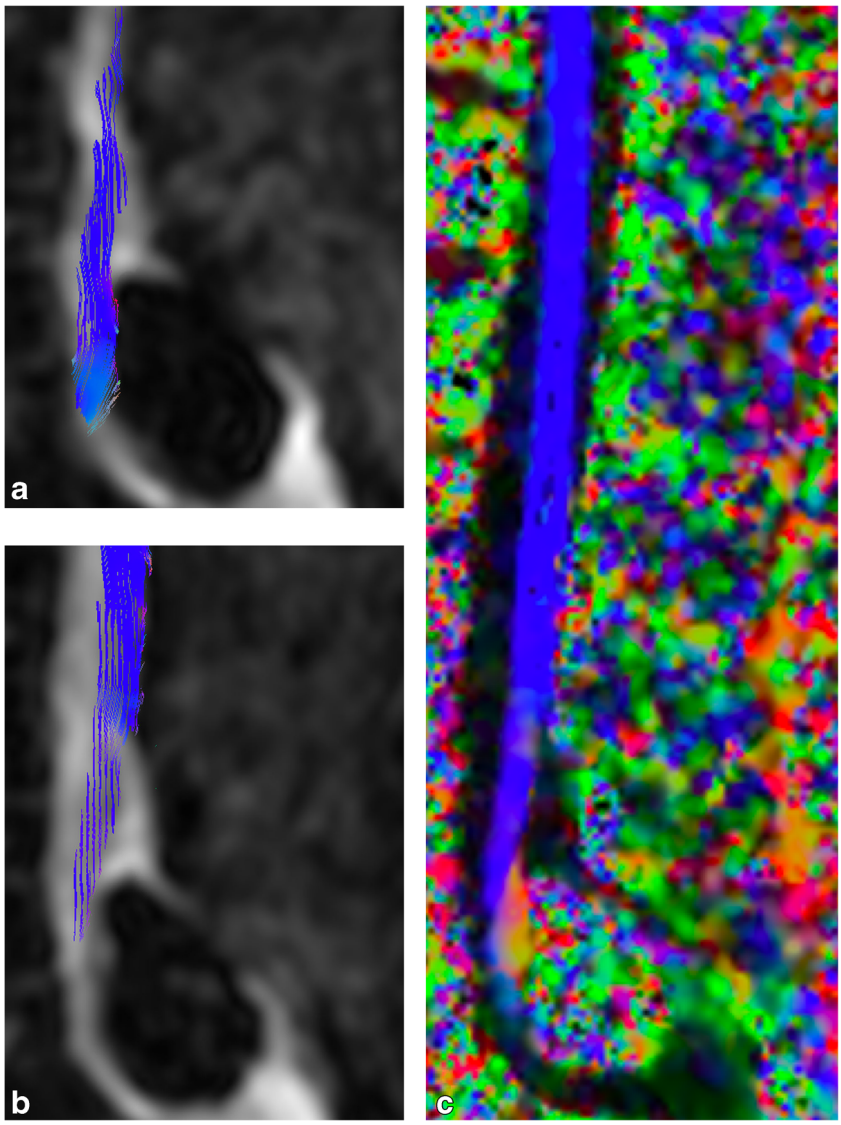

Fig. 3 **a**, **b** Tractography reconstruction of the conus medullaris of patient 8 (male, 39 months old). **c** Sagittal color FA mapping

measurements on the quality and especially the average quantity of fibers reconstructed according to clinical presentation and natural history of the patients.

There are indeed many DTI studies reported in the literature that have investigated the cervical spinal cord in healthy or in traumatic cases in both, the adult and pediatric population [10]. In these studies, the authors have developed some indices (tract density indice for example) related to the density of the fibers within the white matter of the spinal cord that are defined per voxel as in the brain [26]. They have demonstrated that the spinal cord compression or spinal cord injury, by compression or other types of trauma mechanisms, resulted in a decrease of the indices and therefore refers to a destruction of fibers [27]. Due to limits of our study, we would not directly compare our results to those reported literature. However, the use of indices for the density in SL could probably represent a significant prognostic factor predicting the clinical and postoperative outcome.

We have shown that tractography of the conus medullaris in the pediatric population with SL is possible, reproductive, and allows visualization of the spinal cord within this dysraphism. In the close future, we will propose a prospective study and developing and applying these types of indices in SL and more widely in dysraphisms. This work shows that tractography allows the visualization of the medullary cone. In a future study, this may be interesting when classical MRI techniques do not allow knowing the macro-architecture, in complex dysraphisms, especially in complex forms of myelomeningoceles.

Compliance with ethical standards

Conflict of interest We declare that we have no conflict of interest to declare.

References

1. Mitchell JB, Pang D (2008) Surgical management of spinal dysraphism. Operative Technique in Pediatric Neurosurgery 2(60):707–734
2. Pierre-Kahn A, Zerah M, Renier D (1995) Lipomes malformatifs intrarachidiens. Neurochirurgie 41(Supp 1):1–134
3. Zerah M, Roujeau T, Catala M, Pierre-Kahn A (2008) Spinal Lipomas. In: Spina Bifida, Management and Outcome. pp 445–474
4. Basser PJ, Mattiello J, LeBihan D (1994) Estimation of the effective self-diffusion tensor from the NMR spin echo. J Magn Reson B 103:247–254
5. Douek P, Turner R, Pekar J, Patronas N, Le Bihan D (1991) Mr color mapping of myelin fiber orientation. J Comput Assist Tomogr 15(6):923–929
6. Tournier JD, Mori S, Leemans A (2011) Diffusion tensor imaging and beyond. Magn Reson Med 65(6):1532–1556
7. Khalil C, Hancart C, Le Thuc V, Chantelot C, Chechin D, Cotton A (2008) Diffusion tensor imaging and tractographie of the median nerve in carpal tunnel syndrome: preliminary results. Eur Radiol 18(10):2283–2291
8. Wieshmann UC, Clark CA, Symms MR, Franconi F, Barker GJ, Shorvon SD (1999) Reduced anisotropy of water diffusion in structural cerebral abnormalities demonstrated with diffusion tensor imaging. Magn Reson Imaging 17(9):1269–1274
9. Mori S, van Zijl PC (2002) Fiber tracking: principles and strategies—a technical review. NMR Biomed 15(7–8):468–480
10. Clark CA, Werring DJ (2002) Diffusion tensor imaging in spinal cord: methods and applications—a review. NMR Biomed 15(7–8): 578–586
11. Maier SE, Mamata H (2005) Diffusion tensor imaging of the spinal cord. Ann N Y Acad Sci 1064:50–60
12. Filippi CG, Andrews T, Gonyea JV, Linnell G, Cauley KA (2010) Magnetic resonance diffusion tensor imaging and tractography of the lower spinal cord: application to diastematomyelia and tethered cord. Eur Radiol 20(9):2194–2199
13. Tsuchiya K, Fujikawa A, Honya K, Nitatori T, Suzuki Y (2008) Diffusion tensor tractography of the lower spinal cord. Neuroradiology 50(3):221–225
14. Sysoev KV, Tadevosyan AR, Nazinkina YV, Khachatryan VA (2016) (2016) Surgical treatment outcomes in children with tethered spinal cord syndrome. A prognosis on the basis of spinal 3T MRI tractography. Zh Vopr Neirokhir Im N N Burdenko 80(3):66–73
15. Haakma W, Dik P, ten Haken B, Froeling M, Nievelstein RA, Cuppen I, de Jong TP, Leemans A (2014) Diffusion tensor magnetic resonance imaging and fiber tractographie of the sacral plexus in children with spina bifida. J Urol 192(3):927–933
16. Saksena S, Middleton DM, Krisa L, Shah P, Faro SH, Sinko R, Gaughan J, Finsterbusch J, Mulcahey MJ, Mohamed FB (2016) Diffusion tensor imaging of the normal cervical and thoracic pediatric spinal cord. AJNR Am J Neuroradiol 14
17. Toussaint N, Souplet JC, and Fillard P (2007) MedINRIA: medical image navigation and research tool by INRIA. In proc. of MICCAI '07 workshop on interaction in medical image analysis and visualization. Brisbane Australia
18. Fillard P, Pennec X, Arsigny V and Ayache N (2007) Clinical DT-MRI estimation, smoothing and fiber tracking with log-Euclidean metrics Asclepios Reseach Team, INRIA Sophia Antipolis
19. Middleton DM, Mohamed FB, Barakat N, Hunter LN, Shellikeri S, Finsterbusch J, Faro SH, Shah P, Samdani AF, Mulcahey MJ (2014) An investigation of motion correction algorithms for pediatric spinal cord DTI in healthy subjects and patients with spinal cord injury. Magn Reson Imaging 32(5):433–439
20. Barakat N, Mohamed FB, Hunter LN, Shah P, Faro SH, Samdani AF, Finsterbusch J, Betz R, Gaughan J, Mulcahey MJ (2012) Diffusion tensor imaging of the normal pediatric spinal cord using an inner field of view echo-planar imaging sequence. AJNR Am J Neuroradiol 33(6):1127–1133
21. Wang K, Song Q, Zhang F, Chen Z, Hou C, Tang Y, Chen S, Hao Q, Shen H (2014) Age-related changes of the diffusion tensor imaging parameters of the normal cervical spinal cord. Eur J Radiol 83: 2196–2202
22. Dubois J, Dehaene-Lambertz G, Perrin M, Mangin JF, Cointepas Y, Duchesnay E, le Bihan D, Hertz-Pannier L (2008) Asynchrony landmarks revealed noninvasively by diffusion tensor imaging. Hum Brain Mapp 29(1):14–27
23. Baumann N, Pham-Dinh D (2001) Biology of oligodendrocyte and myelin in the mammalian central nervous system. Physiol Rev 81: 871–927
24. Langworthy OR (1933) Development of behavior patterns and myelinization of the nervous system in the human fetus and infant. Contributions of Embryology of the Carnegie Institution 24:3–57
25. Kubis N, Catala M (2003) Development and maturation of the pyramidal tract. Neurochirurgie 49(2–3 Pt 2):145–153
26. Haynes WIA, Clair AH, Fernandez-Vidal S, Gholipour B, Morgiève M, Mallet L (2018) Altered anatomical connections of associative and limbic cortico-basal-ganglia circuits in obsessive-compulsive disorder. Eur Psychiatry 51:1–8
27. Alizadeh M, Fisher J, Saksena S, Sultan Y, Conklin CJ, Middleton DM, Finsterbusch J, Krisa L, Flanders AE, Faro SH, Mulcahey MJ, Mohamed FB (2018) Reduced field of view diffusion tensor imaging and fiber tractography of the pediatric cervical and thoracic spinal cord injury. J Neurotrauma 35(3):452–460
28. Singhi S, Tekes A, Thurnher M, Gilson WD, Izbudak I, Thompson CB, Huisman TAGM (2012) Diffusion tensor imaging of the maturing paediatric cervical spinal cord: from the neonate to the young adult. J Neuroradiol 39:142–148
29. Kulkarni AV, Pierre-Kahn A, Zerah M (2004) Conservative management of asymptomatic spinal lipomas of the conus. Neurosurgery 54(4):868–875